January 17, 2010

Dr. Jon Nakane,
University of British Columbia
Department of Physics and Astronomy
6224 Agricultural Road,
Vancouver, British Columbia, Canada
V6T 1Z1

Dear Dr. Nakane,

We are submitting to you our final recommendation report which follows from our APSC 479 project work. The project goal was to optimize microwave antennas to be used in Rubidium quantum spin manipulation experiments by Dr. Kirk Madison et al in the Quantum Degenerate Gas laboratory (University of British Columbia, Physics Department). The designed antennas improve upon previous prototypes by achieving greater radiation directivity and gain. The report outlines the project background and motivation, discusses the project completion, and concludes with future design recommendations.

Sincerely,

Taylor Dean
Engineering Physics
University of British Columbia
tdeaner@interchange.ubc.ca

Dan Crawford
Engineering Physics
University of British Columbia
shekler@interchange.ubc.ca

Microwave Antenna Design for Quantum Spin Manipulation of Laser Cooled Rubidium Atoms

Taylor Dean
Daniel Crawford

Project Sponsor:
Dr. Kirk Madison
Quantum Degenerate Gases Laboratory
University of British Columbia

Applied Science 479
Engineering Physics
University of British Columbia
January 17, 2010

Project Number 964

Executive Summary

The objective of this project is to design a set of highly directive microwave antennas: one operating near 6.8 gigahertz and the other at 3.0 gigahertz. These antennas are to be used in a controlled laboratory experiment to manipulate the quantum spin of laser cooled rubidium atoms. The atoms have an associated magnetic dipole, allowing their spin to be altered with the application of resonant microwaves.

Initially, two fabricated antenna prototypes were available: one dipole and one helix. These first generation designs have been characterized by exploring frequency dependencies and spatial emission patterns. It is found that the helical antenna is more directional than the dipole, and is thus chosen as the final design type. The frequency response of the helical antenna shows a peak gain of 6.0 GHz. This peak allows the calculation of the dielectric constant of Delrin, the core material. The physical parameters of the helix (circumference, number of turns, length and dielectric material) are then manipulated to guarantee that the peak intensity can be achieved at either 6.8 GHz or 3.0 GHz. The core dielectric material of the next generation prototypes remains Delrin, since its behaviour is now well documented and the cost is minimal.

Aside from experimental results, two methods of increasing helical antenna directionality and gain have been researched and implemented in the final design. Four helical antennas will be placed in an array, which leads to much higher directionality and a lower input impedance. Parasitic antennas have been added in Helix-Helix formation around each antenna in the array. These extra elements reduce radial radiation bleeding and direct stray wave axially.

The next generation antennas are currently under construction in the University of British Columbia Physics and Astronomy machine shop and will be available for construction and characterization within the first quarter of 2010.

Table of Contents

List of Figures

List of Tables

1. Background and Motivation

This project focuses on the design of optimized microwave antennas used in experiments intended to manipulate the spin of ^{85}Rb and ^{87}Rb atoms. Two prototypes, a dipole antenna and a helical antenna, were available for characterization to aide in the development of a final design. The initial antennas were characterized in terms of frequency variation on a range of approximately ±2GHz and for the spatial distribution of intensity. Once baseline data for each prototype was collected and analyzed, the final version could be created. The final model will, ideally, exhibit high directionality at the specified frequency. The experimental set-up necessitates that the antennas be as small as possible in order to be placed in close proximity to the Rubidium Dipole Trap. Furthermore, the project sponsors required a final antenna design with a well-defined and well-documented fabrication process in order to construct additional copies in the future.

The project sponsor is Dr. Kirk Madison of the Quantum Degenerate Gases (QDG) Laboratory at the University of British Columbia. Additional guidance and supervision was provided by Dr. Benjamin Deh, also of the QDG group. This report is produced to provide a summary and analysis of the collected prototype antenna data and a description of the final design.

1.1 Experiment Background

The experimental set-up used by the QDG lab consists of the Rubidium State Selector (RbSS), microwave antenna, and Rubidium Dipole Trap, as well as many other commercial measurement devices. This report provides and overview of the RbSS operation and microwave antenna analysis and design as only these two aspects were studied during the course of the project[1].

The overall experiment is designed to emit microwave radiation at one of two frequencies: 6.8 GHz and 3.0 GHz. 6.8 GHz is the Feshbach resonance frequency for ^{87}Rb and 3.0 GHz is the Feshbach resonance frequency for ^{85}Rb. Using these frequencies, the quantum states of the atoms may be manipulated. Feshbach resonance is used to increase the interaction rate between atoms and has various applications including Bose Einstein Condensates and accurate measurements of magnetic fields. The QDG team is particularly interested in studying interactions between Rubidium and Lithium atoms. The design of an optimal antenna to transfer intensity accurately and efficiently from the RbSS to the Rubidium Dipole Trap will improve the quality of the current experimental set-up.

[1] More information on the overall experiment is available in Alan Robinson's report: *Measuring the Molecular Structures of Ultracold Lithium-Rubidium Dimers by Feshbach Resonances* – University of British Columbia, June 2009.

1.2 Initial Prototypes

Two initial prototypes were available at the beginning of the project. These versions were to be tested and analyzed to generate baseline comparison data. Because there are many antenna architectures including dipole, helical, parabolic, horn, etc, another function of testing the two original models is to aide in determining the final antenna type. One model available for characterization is a dipole antenna and the other is a helical antenna. Both tested models were designed to emit radiation at 6.8 GHz, although third dipole antenna model, which was designed at 3.0 GHz, exists and was in use in experiments during the term of the project.

The dipole antenna is the first prototype antenna, shown in Figure 1[2], and was constructed for the initial experiment. It has a reflector behind the antenna to increase the directivity and match the impedance to 50Ω. Previous calculations and measurements show the impedance is 50Ω, and the Voltage Standing Wave Ratio (VSWR) is 1.03 for the 3.0GHz antenna and 1.19 for the 6.8GHz dipole antenna (1). An in-depth description of this antenna, including directivity plots, if available in Allan Robinson's report: *Measuring the Molecular Structure of Ultracold Lithium-Rubidium Dimers by Feshbach Resonances* – University of British Columbia, June 2009 (1).

Figure 1
6.8GHz dipole antenna

[2] Taken from Alan Robinson's report: *Measuring the Molecular Structures of Ultracold Lithium-Rubidium Dimers by Feshbach Resonances* – University of British Columbia, June 2009

Even with the reflector, the dipole antenna version may not provide the maximum directivity. Thus, the helical antenna was created as the next version of the antenna. Certain constraints resulted in an intermediate version of the helical antenna with a makeshift ground plane, shown in Figure 2[3]. Testing with this model provided unsatisfactory results, which were thought to result from an incorrect dielectric constant estimation or poor impedance matching (2). The newest prototype version has the machined ground plane, shown in Figure 3. This is the version which was tested, along with the original dipole antenna, for the duration of the project.

Figure 2
6.8GHz helical antenna with make-shift ground plane

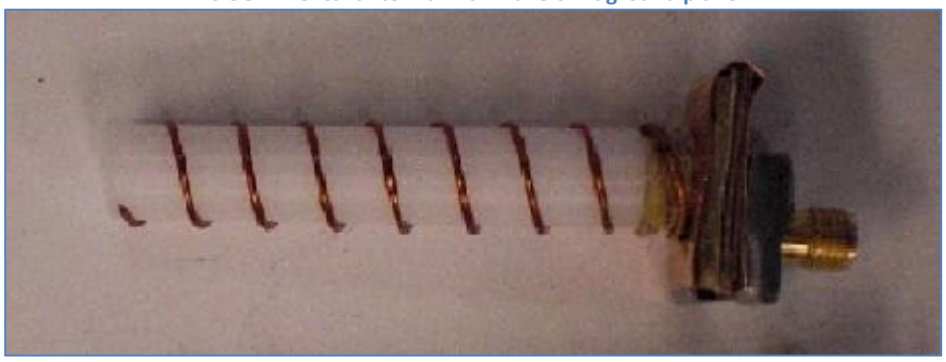

Figure 3
6.8GHz helical antenna with fabricated ground plane and Delrin Shell

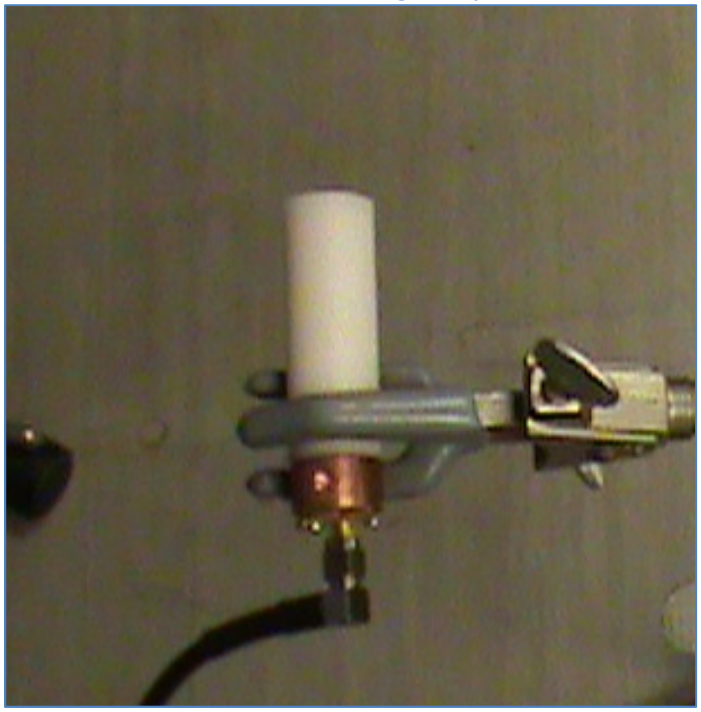

[3] Taken from Theo Rybarczyk's report: *Microwave system for ^{85}Rb and ^{87}Rb hyperfine transitions and Feshbach resonances* – University of British Columbia

The helical antenna's dimensions are easily altered through the use of a dielectric core. An initial problem with the helical antenna was the antenna length, as a small antenna is required for the experiment. As an example, the 3.0GHz model had a calculated length of 22.2cm for a helical loop in a vacuum. The required length of the helix is proportional to the wavelength; therefore it may be reduced by having a core and shell material with a large dielectric constant.

1.3 Technical Requirements

As stated above, the antenna must exhibit high directivity and be as small and robust as possible. There is no stated minimum length or size for the antenna. The objective of the project is to balance size and intensity to create an antenna which will transfer maximum radiation to the Rubidium Dipole Trap as efficiently as possible. The size of the antenna can be quantified by viewing the source field from the dipole trap. The solid angle created by the antenna takes into account both the size of the antenna and the distance from the dipole trap. Therefore, the solid angle should be taken into account when quantifying the final version.

One specification which arises from the project outline is the aspect of impedance matching. To transfer the microwave signal efficiently, the microwave antenna should have 50Ω input impedance. This is especially an issue in the case of the helical antenna, where the input impedance is directly proportional to the helix circumference. This is discussed more in the theory segment of the discussion section.

Another technical requirement, which is mostly for ease of integration into the existing system, is the use of SMA connections between the antenna and RbSS. SMA connectors also have a 50Ω input impedance and perform adequately in the 3.0GHz and 6.8GHz range. Both the existing dipole and helical antennas were designed with SMA connections, as is the final design.

1.4 Industrial Competitors – Alternative Strategies

Fractal Antenna Systems Inc. design and manufacture antennas for commercial, military, and government applications. Fractal Antenna Systems designs antennas using fractal geometry, enabling them to manufacture antennas which are 50 to 75 percent smaller than traditional antennas (3). Furthermore, using fractal geometry allows for a higher number of resonant frequencies than traditional antenna designs. Furthermore, Fractal Antenna Systems has a comprehensive design process in which its team of engineers conducts works with the customer from the project definition to the product production phase. This company was not pursued as a possible source of microwave antenna fabrication due to time and cost constraints.

Other options for the final design included selecting from any of the various antenna types. The project goal was to test and characterize the existing prototypes and use the data to generate an optimal final design. Therefore, it did not appear to be in the best interest of the team to develop a third prototype of an entirely different design such as horn, parabolic, or spiral, which would then have to be tested, characterized, compared, and fine-tuned before an optimal version is produced.

2. Discussion

The following sections outline the project objectives, technical background and theory, methods and experimental set-up, and final designs.

2.1 Project Objectives

The project objectives for this project include characterizing the current antenna designs, researching alternate antenna types and materials, establishing a final design, and determining characteristics of the final antenna. These are described in more detail in the following sub sections.

Objective 1: Characterization of Existing Antennas

There are currently two antennas available for characterisation. The first is a dipole antenna which has already undergone testing, although the tests will be repeated by the team for project consistency. The team will measure the antennas impedance, reflectance, and emission pattern. The emission pattern for antennas can be characterized in terms of two quantities: the gain and the intensity distribution. The second prototype is a helical antenna with a Delrin core. Similarly to the dipole antenna, the team will measure the antenna impedance, reflectance, and emission pattern. In addition to these parameters, the exact dielectric constant of Delrin at both 3.0GHz and 6.8GHz must also be determined.

Objective 2: Research Alternate Designs and Materials

There are many types of antennas, including dipole, helical, biconical, sleeve, and spiral, as well as many ways of fabricating each (see section on Fractal Antenna Systems, above). The various antenna type and fabrication options will be researched in order to determine which antenna is optimal for the specific experiment. The deliverable for this objective will be to establish an ideal shape, material, and fabrication process for the antenna in order to begin working on a final design.

Objective 3: Establish Final Design

A final design for an optimal antenna which is both robust and reproducible is required for Objective 3. This includes placing all orders for parts and materials, as well as all submitting machine shop work orders. Drawings must be completed to provide the machine shop with an outline of the antenna shape and to help with antenna fabrication.

Objective 4: Characterizing the Final Antenna

The final version of the antenna must be characterized in the same manner as the prototypes. The team will measure the antenna impedance, reflectance, and emission pattern. Any unforeseen changes to the antenna design should be accounted for in a new drawing set for the final design package.

2.2 Technical Background and Theory

This section outlines the additional theory required to describe the project, which has been developed in the time proceeding the initial project proposal.

2.2.1 Helical Antennas: Theory of Antenna Arrays and Parasitic Antennas

As mentioned in Objective 2 of the project objectives section above, the team is to research alternate designs to improve antenna gain and directionality. It is the opinion of the team that the helical antenna gives the greatest directionality and intensity when operated in its axial mode. In this context, axial mode implies that the radiation pattern is parallel to the helical axis, having the maximum of the radiated power in the direction of cylinder axis. A literature search has shown that there are two common methods to further increase the gain and directionality of the helical antenna: creating symmetric antenna arrays and modifying winding design to include parasitic antennas.

Arrays of Monofilar Axial-Mode Helical Antennas

The novelty behind the array of monofilar axial-mode helical antennas is that it maintains the single antenna emission pattern characteristics (highly directional radiation emission pattern) while increasing the gain. A diagram showing how the array is arranged is shown below in Figure 4.

Figure 4
The 2 by 2 Antenna Array front view (left) and side view (right). A1, A2, A3 and A4 represent individual helical antenna elements and d is the displacement between them. The antennas are mounted on a reflecting back-plate.

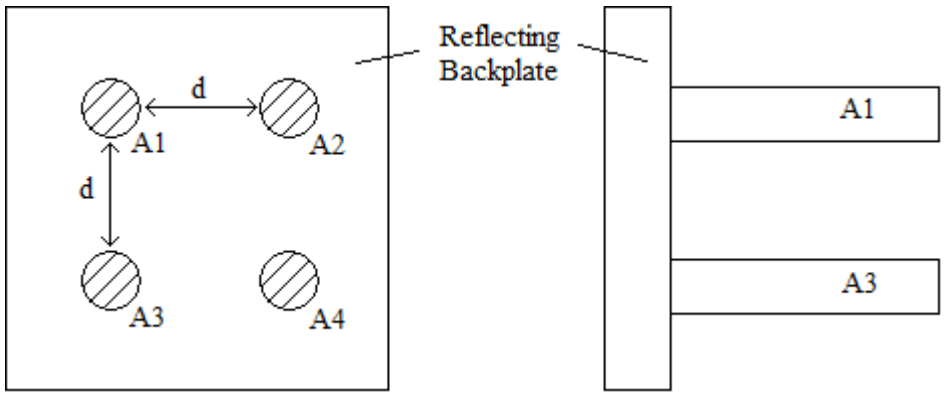

Let the desired output wavelength of the system to be λ. The distance between adjacent antennas in the 2 by 2 system have been experimentally been chosen to be 1.5 λ (4), both horizontally and vertically (d = 1.5 λ). This configuration produces the most symmetry of the main lobe in both **E** and **H** polarizations, yielding maximum directional gain.

After measuring the output radiation pattern of a single helical antenna (which has been done during the course of this project), we obtain an emission pattern R(r, θ, ϕ). To demonstrate the effect of the array, the antenna array factor for N antenna elements $(AF)_N$ must be defined.

Given R(r, θ, ϕ), the emission pattern of the array can be approximated (to within 20%) by

$$y(\theta,\varphi) = R(\theta,\varphi)\,(AF)_N$$

Where, for a uniformly spaced N element array,

$$(AF)_N = \left[\frac{\sin\left[\frac{N}{2}kd(cos\theta-1)\right]}{N\sin\left[\frac{1}{2}kd(cos\theta-1)\right]}\right]$$

Here, k is the wave number and d is the distance between array elements.

Therefore, for the N=4 array designed for this project,

$$(AF)_3 = \left[\frac{\sin[2kd(cos\theta-1)]}{3\sin\left[\frac{1}{2}kd(cos\theta-1)\right]}\right]$$

And

$$y(\theta,\varphi) = R(\theta,\varphi)\left[\frac{\sin[2kd(cos\theta-1)]}{4\sin\left[\frac{1}{2}kd(cos\theta-1)\right]}\right]$$

From this it is apparent the maximum radiation intensity still occurs along the axis θ = 0°.

To further prove that directionality is improved using the array, the directionality of the N=1 element and the N=4 element array will be compared.

The measure of directionality of a single helix is given by

$$D_{o,single} \approx 12n\frac{C^2S}{\lambda^3}$$

Where n is the number of turns in the helix, S is the spacing between two adjacent windings and C is the circumference of a single turn. The implemented design (f = 6.8 GHz) has n = 8, C = 0.06 m, and S = 0.006 m giving $D_{o,single} \approx 24.1$.

The directionality of the 2 by 2 array is given by

$$D_{0,array} = \frac{U_{max}}{U_o}$$

Where U_{max} is the maximum intensity value of y(θ,ϕ) and is taken to be 1 and $U_o \approx \frac{\pi}{2Nkd}$

Therefore,

$$D_{0,array} \approx \frac{2Nkd}{\pi} = 4N\left(\frac{d}{\lambda}\right) = 4\left(1+\frac{L}{d}\right)$$

Or by implementing the Hansen-Woodyard approximation for antenna arrays, the directivity is given by

$$D_{0,array} = \frac{U_{max}}{U_o} = \frac{1}{0.554}\left[\frac{2Nkd}{\pi}\right] = 1805\left[4N\left(\frac{d}{\lambda}\right)\right]$$

Given N = 4, d = 1.5λ: $D_{0,array} \approx 43300$

So it has been shown that $D_{0,array}$ >> $D_{0,single}$ and the use of the array is justified and beneficial for large directionality increases.

To address gain increases, it must be indicated that each element of the array has an associated - and approximately identical – impedance Z, and by the law of adding parallel impedances the impedance of the N=4 array is given by

$$Z_{array} = Z||\mathrm{Z}||\mathrm{Z}||\mathrm{Z} = \frac{\mathrm{Z}}{4}$$

So the array impedance of the array is one quarter that of a single antenna, which given a constant source power input, will yield a higher output gain.

In conclusion, the helix-antenna array will generate an output which is more directional and has a higher gain than that of a single antenna element. If the array does not break the solid angle constraints needed for the project sponsor's optical arrangement, this option will be a significant improvement on the original antenna design.

Helix-Helix Parasitic Elements

A parasitic antenna (or passive radiator) is a radio antenna which is not connected to its source by a wire. This added element absorbs radiation from surrounding antennas and re-radiates it, which leads to higher directionality and thus higher intensity in the axial direction. During spatial emission pattern characterization experiments, it was noticed that there was a significant amount of radiation produced non-axially. This added element will redirect a portion of this radiation and force it to propagate axially. Figure 5 below shows how the parasitic element will be placed with respect to the original helical antenna.

Figure 5

Helix-Helix parasitic antenna element. The Driven Antenna (red) is powered directly from the RbSS, and the Parasitic Antenna (blue) is not powered, but rather directs the non-axial radiation from the Driven Antenna, increasing directionality.

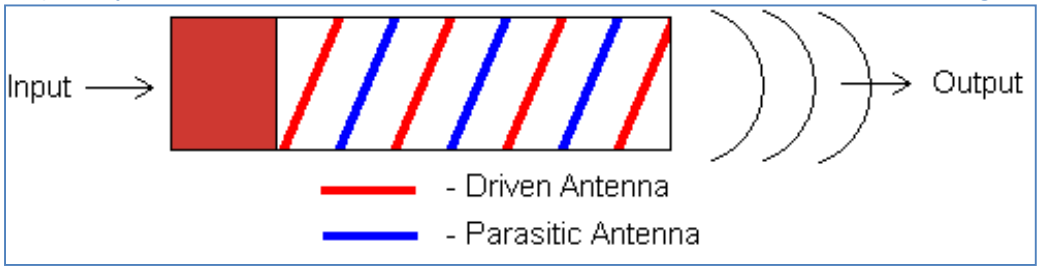

John D. Kraus, the inventor of the helical antenna, reports the following in his textbook Antennas 2nd Ed. (1988) on the gain increase and improved directionality of this helix-helix parasitic antenna modification (5):

"If a parasitic helix is wound between the turns of a driven monofilar axial-mode helical antenna without touching it (diameters the same), Nakano et al. report that the combination gives an increased gain of about 1 dB without an increase in the axial length of the antenna. The increased gain occurs for helices of any number of turns between 8 and 20. The parasitic helix may be regarded as a director for the driven helix."

With these experimentally established advantages of the parasitic helix addition, we have confirmed its use in our final design.

The theory presented by the reference materials for these methods treats helical antenna arrays and parasitic helical antennas separately, i.e., the concept of an array of parasitic helical antennas is not mentioned. Without experimentally quantitatively verifying the performance increases found by combining both methods, it can be loosely argued that having a large reflecting back plate from the antenna array will direct a large portion of the non-axial radiation back toward the parasitic antennas, which trap the waves, re-directing it axially. Likewise for adjacent antennas: each individual helix will emit some radiation radially instead of axially, and there will be three parasitic antennas available to redirect this radiation towards the target.

2.3 Methods and Experimental Equipment

This section focuses on the equipment used to characterize the two prototype antennas. The testing equipment consisted of unique apparatus such as the Rubidium State Selector (RbSS) and antennas, as well as commercial measurement equipment. A DC voltage supply was used to supply power to the RbSS phase locked loop (PLL) and power amplification loop. The reference signal for the PLL was supplied by a function generator, which outputted an 85MHz signal for the 6.8GHz antenna testing. The antenna signal transmitted to the antenna pick-up. A pick-up was assembled at the beginning of the project, however a second pick-up was later used which provided increased signal stability during testing. Figure 6 display the testing set-up used during the project, with standard equipment parameters. The following sections describe the equipment used in the experimental set-up.

Figure 6
Testing set-up for frequency variation and spatial distribution characterization of prototype antennas

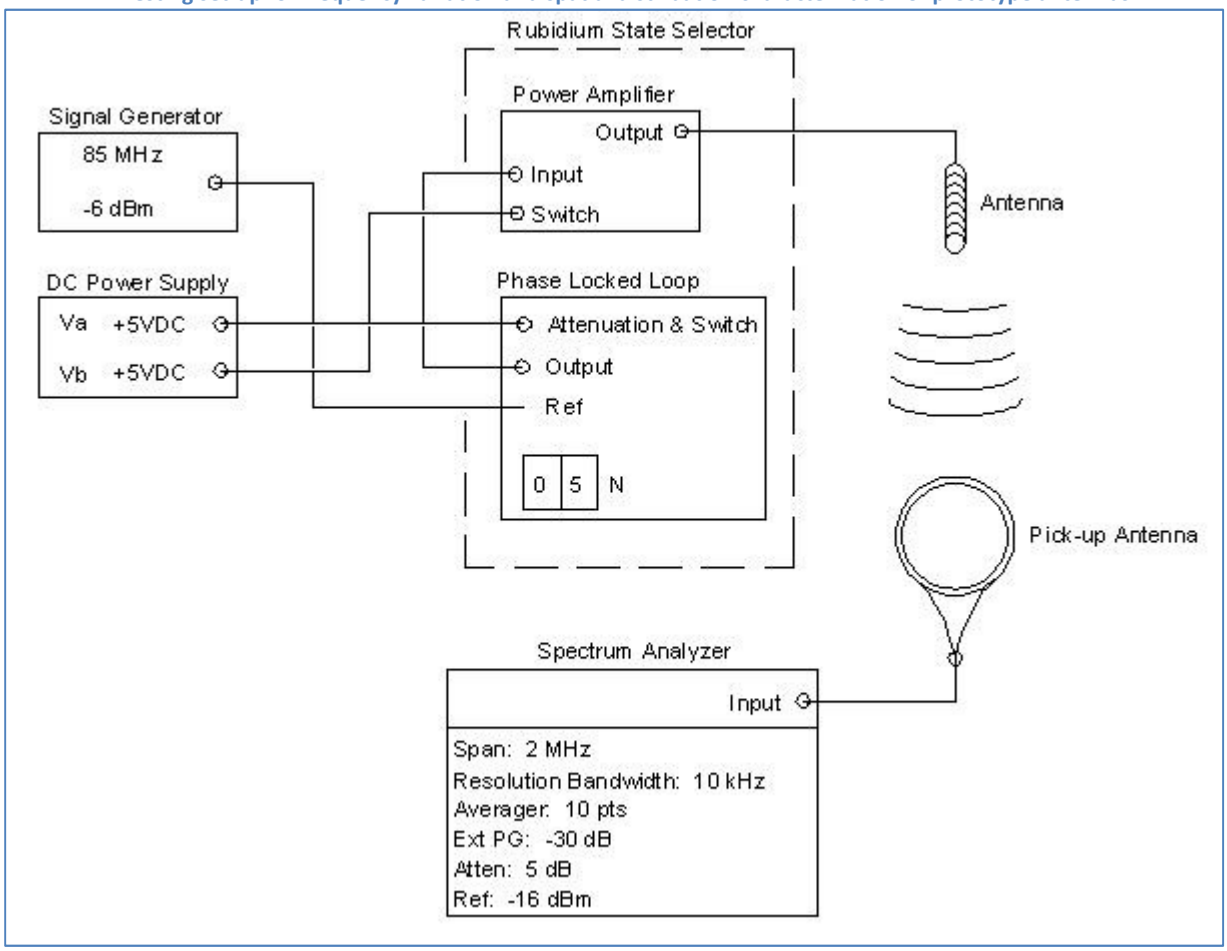

2.3.1 Rubidium State Selector

The Rubidium State Selector consists of a Phase locked loop (PLL) and a power amplification system. Figure 7 shows the RbSS with the power amplifier on the top and the PLL on the bottom. Both the PLL and power amplification loop require DC signals in order to function. The PLL has a "attenuation and switch" input which is connected to +5VCD, and the power amplification loop has a "switch" label which is also connected to +5VDC.

Figure 7
Rubidium State Selector, consisting of a phase locked loop and power amplifier.

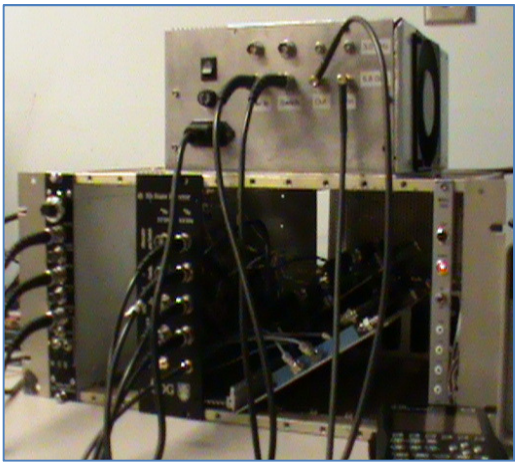

The purpose of the PLL is to control the output frequency of the voltage controlled oscillator (VCO). The VCO output is first frequency divided and compared with a reference voltage signal from a signal generator. A DC servo signal is produced and used as feedback to adjust the voltage applied to the voltage controlled oscillator. Thus, the VCO is locked onto the reference signal.

The frequency division occurs to match the frequency range of the VCO with the frequency range of the reference signal from the signal generator. The division constant is adjustable from the front of the RbSS, using a dial to select the value of N. The VCO signal is then divided by 2N. When the VCO is locked to the reference voltage, the output frequency is given by:

$$f_{out} = f_{VCO} = 2Nf_{ref}$$

In both the 6.8 GHz and 3.0 GHz cases, N is set to 5. To obtain the required frequencies, the VCO output is passed through a number of frequency doublers. A reference voltage of 85 MHz along with 3 frequency doublers provides the 6.8 GHz signal, while a reference voltage of 75 MHz along with 2 frequency doublers provides the 3.0 GHz signal. Process diagrams for both signals are shown below in Figure 8.

Figure 8
Process diagram for obtaining the 6.8 GHz (top) and 3.0 GHz (bottom) signals using the PLL and frequency doublers

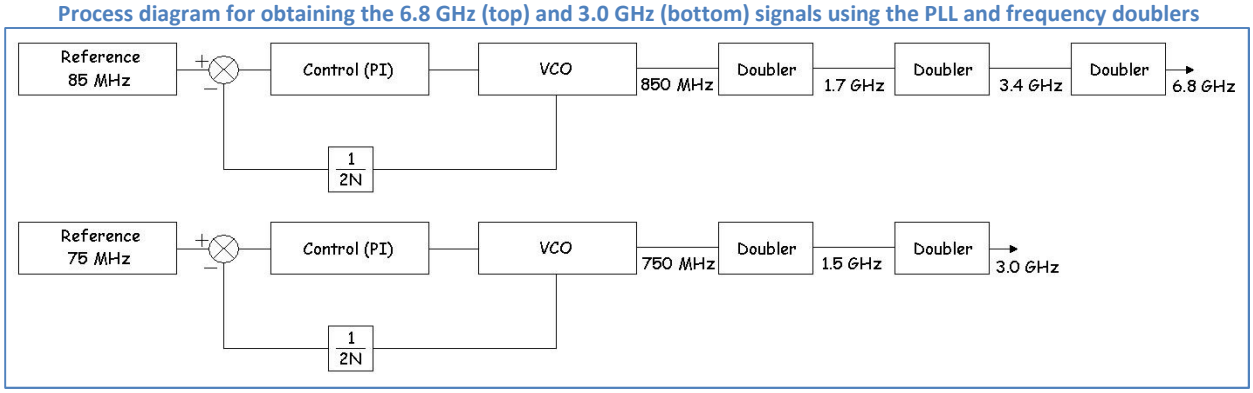

The purpose of the power amplifier is to amplify the signal to around 1W. The output power from the RbSS is controlled with a set-point voltage, supplied by a DC voltage source, which should be between 4V and 10V. The output of the PLL is connected via SMA to the input of the power amplifier, and the output is sent to the antenna. The power amplifier also has a control loop to ensure a constant power output. More information on both the PLL and power amplification loop is found in Theo Rybarczyk's report: *Microwave system for ^{85}Rb and ^{87}Rb hyperfine transitions and Feshbach resonances* – University of British Columbia (2).

One observed issue with the RbSS output is that the output spectrum has additional peaks. Figure 9 below shows the trace data from the spectrum analyzer for an RbSS intended output of 6.8GHz. There is an additional peak, 85MHz below the expected peak, at 5.95GHz. This peak is not expected, and is not seen under the characterization testing span of 2.0MHz.

Figure 9
RbSS trace data from the spectrum analyzer for expected frequency of 6.8GHz, with additional peak at 5.95GHz.

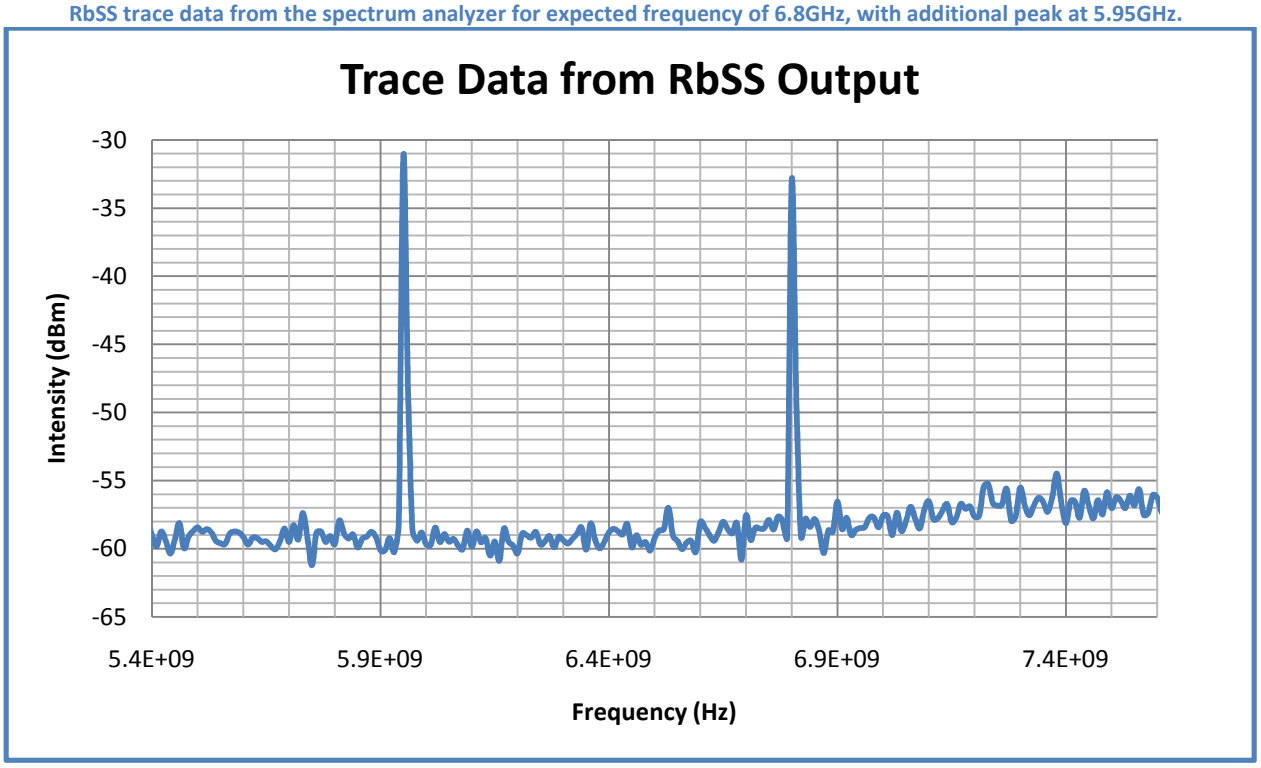

The reference signal required to produce a 6.8GHz signal is 85MHz, which is then multiplied by 10 and doubled 3 times as discussed above. Therefore, the extra peak may be due to defects in the frequency doubler and band-pass filter stages. This result is very reproducible, and because it was not recorded in the spectrum analyzer trace span of 2MHz, it is ignored in the remainder of the report.

2.3.2 Antenna and Pick-up Antenna

The antenna connects to the RbSS through a SMA connection. All versions of the antenna are equipped with SMA connectors to supply the signal. Two pick-up antennas were used in the testing stage, and are displayed in Figure 10. The characterization process included testing the frequency variation at one set distance and orientation as well as a spatial distribution of the intensity pattern. A testing apparatus was assembled using wooden dowels supplied by Dr. Nakane of the Engineering Physics Project Lab, as well as chemistry stands supplied by the QDG lab. The apparatus allows for adjustments of the pick-up relative to the antenna by changing the radial distance and angle. A figure of the antenna and pick-up apparatus is provided in Figure 11.

Figure 10
Two pick-up antennas used in prototype antenna characterization

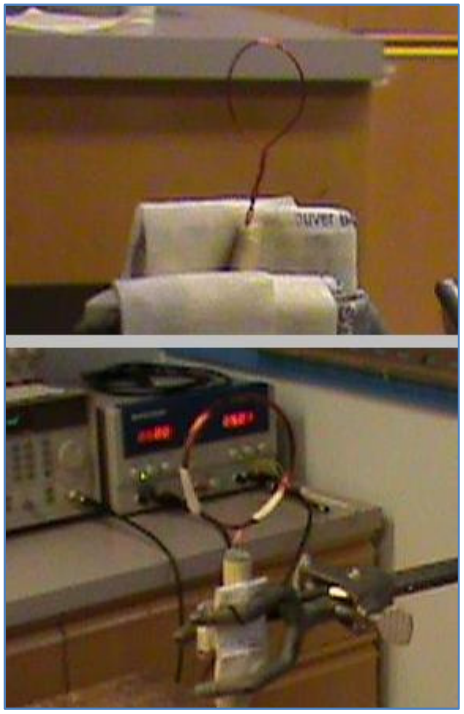

This device was assembled after preliminary testing, when other various changes were made to the experimental set-up. The initial test set-up also utilized chemistry stands to hold the antenna and pick-up, although the system was placed on a table with a marked distance grid for testing. It was hypothesized that some inaccurate values were produced in the initial tests due to reflections off of the table and from the chemistry stand holders. Using marked wooden dowels to measure the distant eliminated the table reflections, although a possible source of error of reflections from the holders remained an issue.

Figure 11
Apparatus to vary antenna and pick-up antenna radial distance and angle

2.3.2 Spectrum Analyzer

The pick-up antenna is connected to the RF spectrum analyzer through a BNC to SMA connector. The analyzer used in the characterization stage was the Agilent E4407-B. Many different tests were conducted with different device values in order to determine the ideal values to generate accurate and reproducible results. Table 1 lists of the parameters used in producing the final data sets.

Table 1
Parameter values for the Agilent E4407-B used to characterize antennas

Parameter	Value
Span	2 MHz
Resolution Bandwidth	10 kHz (auto)
Averager	10 points
Ext PG	-30 dB
Attenuation	5 dB
Reference (Y-axis)	-16 dBm

The spectrum analyzer records trace data over the specified span at the time of data collection. This data is written to a floppy disk in *.CSV* format. The trace data was partially compiled using MATLAB and LabVIEW, and inputted into Microsoft Excel. Each measurement of the frequency variation and spatial distribution characterization stage required a separate trace file. For examples, to test the frequency variation effect for one antenna for ±2GHz at 80MHz intervals required 50 files. Over the course of the experiment this resulted in approximately 500 compiled and analyzed trace files, with 400 data points each.

2.4 Results

To characterize the original antenna prototypes, the team determined the frequency dependencies and the spatially dependent emission patterns of the 6.8 GHz helical and 6.8 GHz dipole antennas. The results of these tests are used to modify the designs to maximize gain and directionality at the desired frequency (6.8GHz or 3.0 GHz). The experiments were performed in the Quantum Degenerate Gas laboratory at the University of British Columbia with the Rubidium State Selector as the source and Agilent Model E4407B radio frequency spectrum analyzer as the measuring receiver.

2.4.1 Frequency Dependency

The frequency study was used to determine the frequency response of each antenna. To maximize gain, the largest intensity amplitudes should lie on the target frequency (6.8 GHz or 3.0 GHz). The frequency dependency of an antenna is dependent on its physical parameters such as winding circumference and core material dielectric constant, so this experiment provides insight into how to alter the design to improve gain.

The frequency experiment was performed on the 6.8 GHz helical and dipole antennas by taking spectrum intensity readings for values between 4.8 GHz and 7.8 GHz in increments of 80 MHz. Both sets of data have been normalized with a baseline dataset taken directly from the Rubidium State Selector. Figure 12 and Figure 13 are a summary of experimental results, as intensity and gain plots respectively.

Figure 12
Intensity vs. Frequency for both the 6.8 GHz helical antenna and the 6.8 GHz dipole antenna

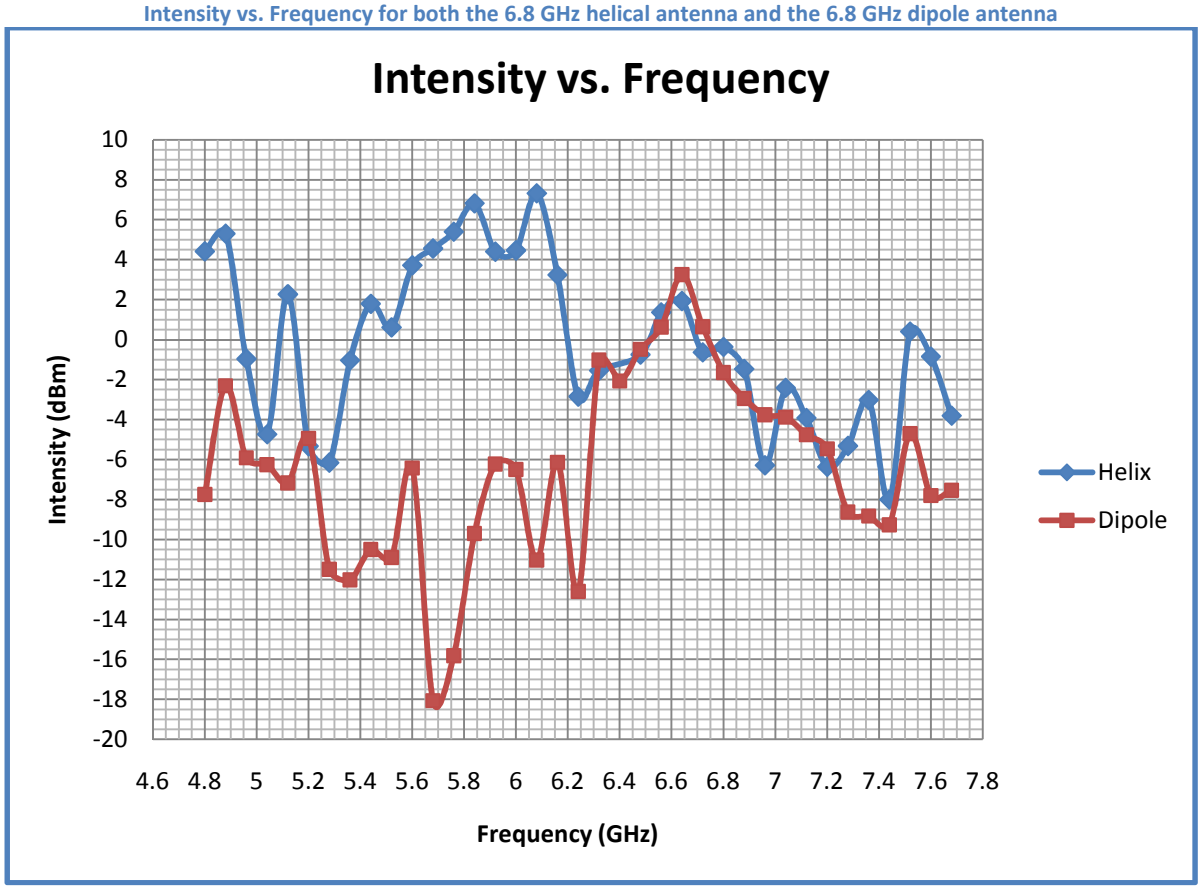

Figure 13
Antenna output gain vs frequency. This further exemplifies the shifted maximum peak of the helical antenna gain.

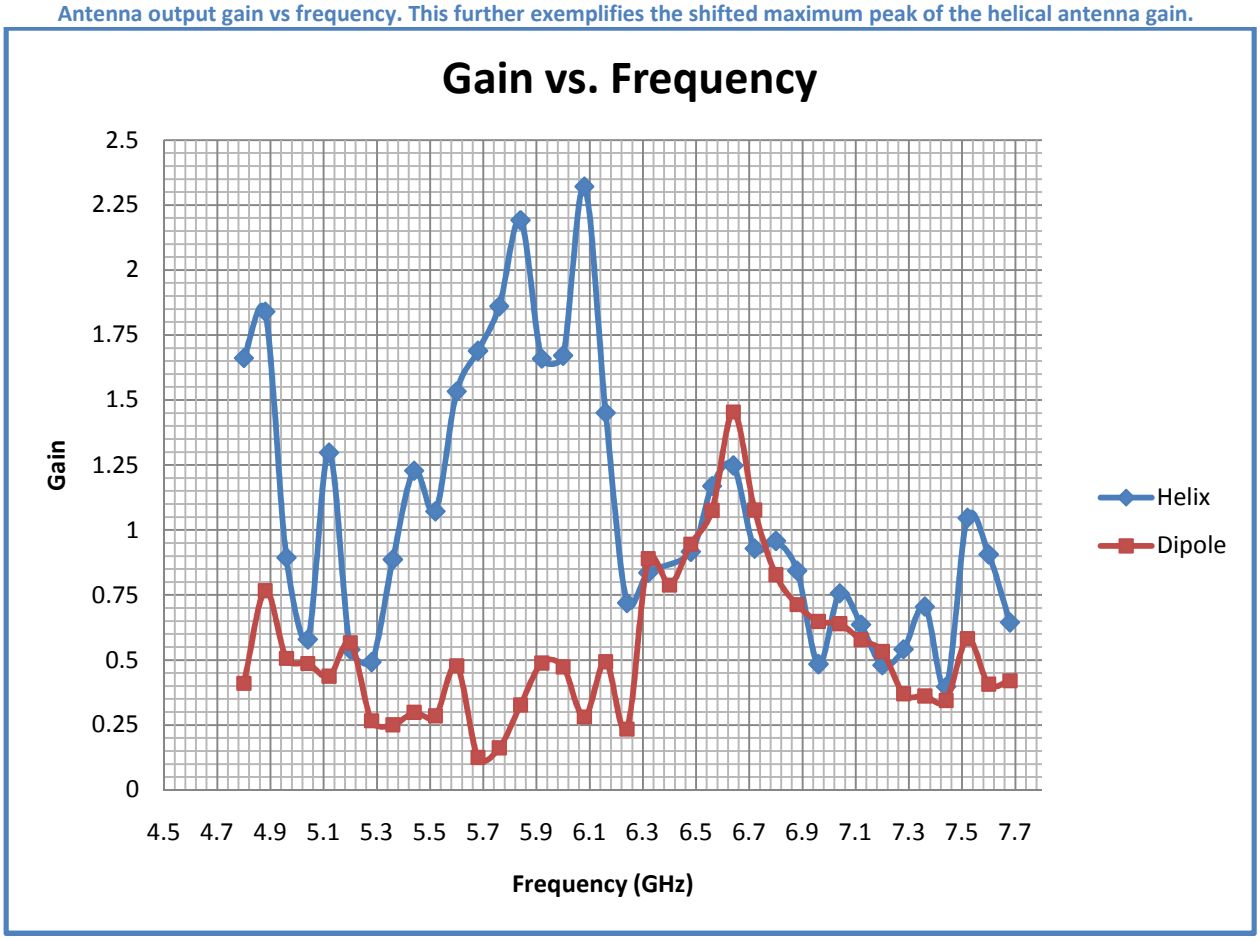

2.4.2 Spatial Emission Pattern

The purpose of the spatial emission pattern experiment is to analyze the antenna directivity and choose a suitable antenna type for the final prototype design. The horizontal plane (i.e., the plane with no vertical antenna emission inclination with respect to the receiving antenna) was decided to be suitable for characterizing spatial intensity dependence. This is a valid generalization because the target for the Rubidium spin manipulation experiment will also lie in this plane (axially, most likely).

Figure 14
Top view of antenna showing sweeping method of measuring planar emission pattern

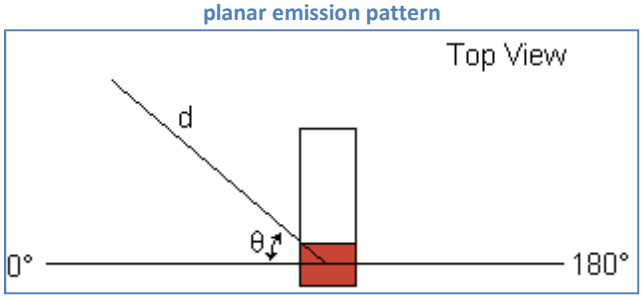

To measure the emission pattern, set displacements were measured at the desired center frequency (6.8 GHz) and at various angles as shown below, to sweep out a plane of data points. Varying angles θ:[0°,180°] in increments of 30°, and varying distances d:[10cm, 100 cm], an array of raw intensity data points were collected. For each antenna the raw intensity data was normalized to the maximum of its set and plotted as a two dimensional contour plots. The results of this experiment are shown below in Figure 15.

Figure 15

Horizontal plane emission patterns. The normalized intensity of the 6.8 GHz helical antenna (left) and the 6.8 GHz dipole antenna (right) have been plotted to compare directivity.

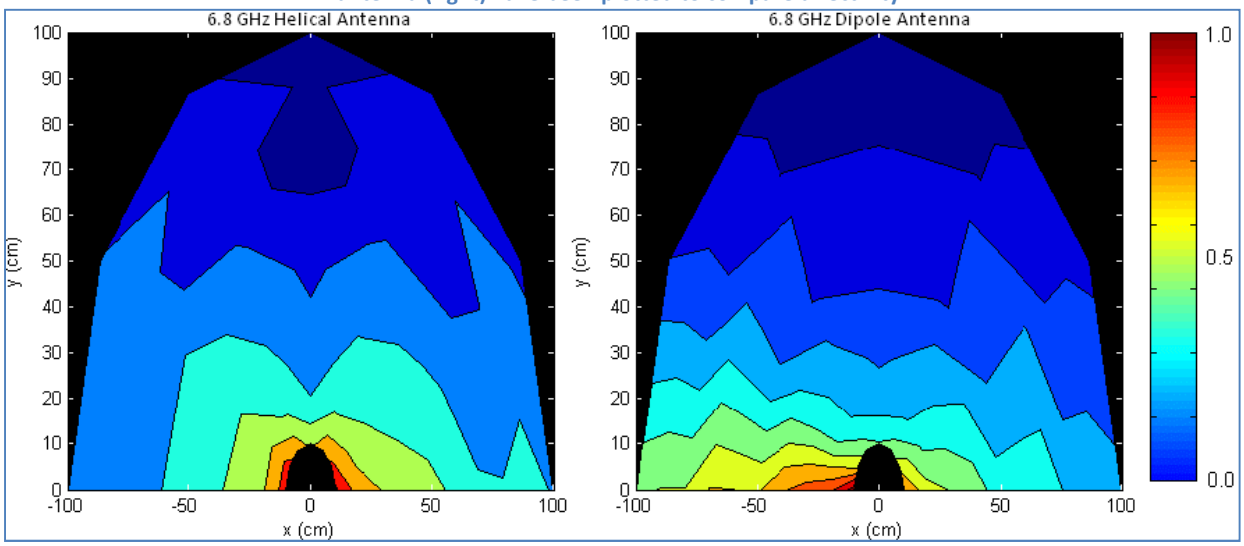

2.5 Discussion of Results

The final antenna prototype designs were decided upon partially by the results of the frequency dependency and spatial emission pattern experiments and also from theoretical models which are described in the theory section of this report. The following sections summarize the important findings of each experiment and what the conclusions have lead to with regard to design alterations.

2.5.1 Spatial Emission Pattern

The spatial emission pattern is used to compare the antenna types. As seen in Figure 15, the dipole antenna bleeds more radiation non-axially close to the antenna output compared with the helical antenna. This characteristic leads to an undesirable lower intensity in the axial direction. When analyzing just the axial emission pattern (the intensity along the vertical line directly above the antenna output), the dipole exhibits large regions of low intensity compared to the helix. These factors have directed the team to choose the helical antenna type for the final prototype.

2.5.2 Frequency Dependency

The results of the frequency dependency experiment strengthen the choice for a helical antenna for the final prototype design. In Figure 13 it is apparent that the gain of the helical antenna is generally higher than the dipole. This is likely due to the radial bleeding described in the section above. The dipole antenna frequency response will not be discussed as the helical antenna proves to be better suited for this application.

Looking now at the helix antenna response, there is a significant rise in gain around 6 GHz, implying that the antenna tested here is not best suited to operate at 6.8 GHz. This frequency response is dependent on the circumference of the helix as well as the dielectric of the core material, and can be altered to perform better at 6.8 GHz in the following way:

The antenna which has been tested operates best at approximately λ_o = 0.05 m and we would like the next prototype to operate at λ = 0.0271 m. In order to achieve axial radiation from a helical antenna must have C and pitch angle α such that

$$\frac{3}{4}\lambda < C < \frac{4}{3}\lambda \qquad \text{And} \qquad 12^o < \alpha < 15^o .$$

The tested antenna has helix circumference C_o = 28mm = 1.2 λ, which is within the required bounds but may be producing the offset. We have therefore chosen to use the midpoint of both the above bounds in an attempt to shift the maximum intensity to λ = 0.0271 m, i.e. C = 1.042 λ and α =13.5°.

To calculate a new circumference we need to know the dielectric constant of delrin ε_r, the core material.

$$\varepsilon_r = \left[\frac{\lambda_o}{\lambda}\right]^2 = \left[\frac{0.050}{0.0271}\right]^2 = 3.4 \pm 0.05$$

Working backwards now using the same dielectric material, set $\lambda = \lambda_o / \sqrt{\varepsilon_r}$, $\lambda_o = c / f$ = 3.0x10^8 / 6.8x10^9, we get λ =0.0239 m and C = (1.042)(0.0239) = 0.025 $\pm$ 0.005 m.

We would like to minimize the length of the antenna and fewer turns will yield a shorter helix. Since N = 8 is the minimum turns required to utilize the parasitic effect, this will be the number of turns for the final design. The length of a single turn is calculated from the pitch angle and circumference:

$$l = C\tan^{-1}(\alpha) = (0.025)\tan^{-1}(13.5^0) = 0.0060 \pm 0.0005m$$

The total antenna length is therefore $L = Nl = (8)(0.0060)$ = 0.048 ± 0.0005 m.

Now knowing the dielectric constant, the same calculations can be performed and a summary of these results can be found in Table 2.

The spatial emission pattern experiment has led to the choice of the helical type antenna for the final design due to the increase in directionality and axial radiation intensity when compared to the dipole antenna. The frequency characterization experiment shows that the first prototype helix is not optimized for 6.8 GHz, but gives us a way to calculate the dielectric constant of Delrin and determine the optimal physical parameters of the antenna to output 6.8 GHz while still having parasitic ability.

2.6 Final Design

As shown in the results section above, the helical antenna exhibited high directivity than the dipole antenna. This was the basis for selecting the helical antenna for the final design. Furthermore, the impedance matching to 50Ω is accomplished though the use of an antenna array system, which in conjunction with the parasitic helix wire will also further increase the directivity. This section contains calculations for the single antenna dimensions as well as descriptions of the parasitic and array antenna structures. Dimensioned drawings are available in Appendix A.

Shown above, the dielectric constant of Delrin, initially thought to be 3.5, is calculated as 3.393. This material was chosen as the final design material due to numerous factors including cost, ease of machining, and because the current Delrin model is already characterized. Other materials are discussed in the Alternative Designs section of the report.

2.6.1 Design Calculations

This section provides an outline of the calculations used in the final design of a Delrin core helical antenna. The wavelength in a vacuum, λ_o, is calculated as:

$$\lambda_0(6.8GHz) = \frac{c_o}{f} = \frac{299792458\ {}^{m}/_{s}}{6.8 \times 10^9 s^{-1}} = 0.04409\ m$$

$$\lambda_0(3.0GHz) = \frac{c_o}{f} = \frac{299792458\ {}^{m}/_{s}}{3.0 \times 10^9 s^{-1}} = 0.1\ m$$

The required circumference of the helix is designed such that it will be in the middle of the circumference range for an axial mode of radiation. Averaging the bounds on the circumference (see Technical Background and Theory section) suggests that the circumference should be 1.042 times the wavelength. The wavelength in the dielectric is scaled by its dielectric constant; therefore, the circumference of both antennas can be calculated from λ_o and the experimentally determined dielectric constant.

$$C_\lambda(6.8GHz) = 1.042(\lambda) = 1.042\left[\frac{\lambda_o(6.8GHz)}{\varepsilon_r}\right] = 0.02494\ m$$

$$C_\lambda(3.0GHz) = 1.042(\lambda) = 1.042\left[\frac{\lambda_o(3.0GHz)}{\varepsilon_r}\right] = 0.05653\ m$$

The circumference values in addition to the selection of the helical pitch angle and number of turns generate values for the helix diameter and length. The pitch angle was selected at 13.5^0 as the average of the upper and lower bounds for an axial mode of radiation. The number of turns was selected at the minimum number of turns in which the parasitic antenna will function to increase the antenna directivity. The helix parameters for the 6.8GHz and 3.0GHz models are shown in Table 2.

Table 2
Parameter values for the 6.8GHz and 3.0GHz helical antennas.

Parameter	6.8 GHz Antenna	3.0 GHz Antenna
Circumference (m)	0.05653	0.02494
Diameter (m)	0.01799	0.00794
Pitch Angle	13.5^{o}	13.5^{o}
Number of Turns	8	8
Length (m)	0.1086	0.04790

2.6.2 Parasitic and Array Antennas

The final design incorporates parasitic antenna and array antenna aspects. These attributes are discussed in the Technical Background and Theory Section of the report. The parasitic antenna can be seen in the single antenna drawing in Figure 16. The difference between this version and the previous helical model is the additional antenna wound between the source helix. This antenna is not connected to the RbSS, and functions only to increase the directivity of the single antenna set-up.

Figure 16
Single helical antenna with parasitic element

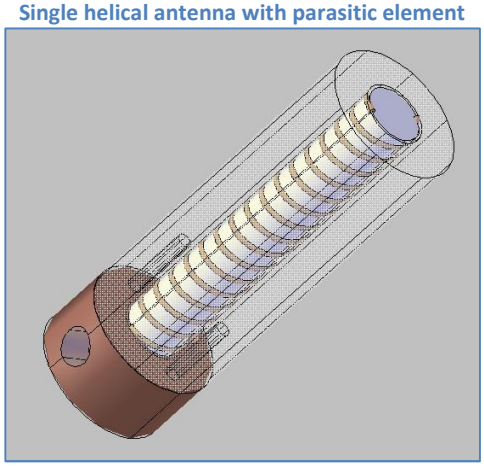

The array antenna structure also functions to increase directivity, but also serves to decrease the input impedance to approximately 50Ω. The array is shown in Figure 17. It is assembled from four single helical antennas spaced at 1.5 wavelengths (1.5λ) in a 2 by 2 grid. The array functions by re-directing any normal mode radiation axially through adjacent antennas (4). The 1.5λ spacing is to ensure the correct phase in the re-direction. The final design will therefore require four antennas for each model (3.0GHz and 6.8GHz), for a total of eight parasitic helical antennas.

Figure 17
Antenna Array Structure

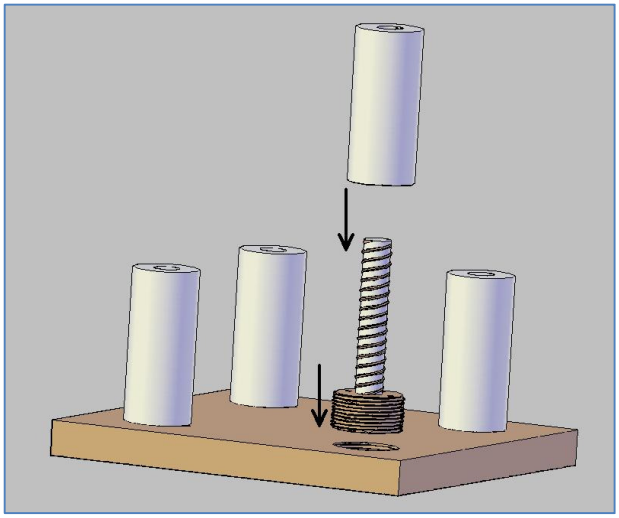

2.7 Sources of Error

Wave Reflections

In experiments measuring antenna radiation characteristics, an ideal laboratory would be large enough to neglect any reflecting waves which may influence intensity measurements. This is not always practical, however, and was not the case during these experiments. The measurements were taken in close proximity to large metal, wood and plastic structures, and how these objects manipulate measurements is still generally unknown. For our purpose (which is to determine emission characteristics of antennas *relative* to one another), ensuring the placement of an antenna within the laboratory was constant for each test allows us to approximately neglect the effects of reflection.

Spectrum Analyzer Resolution Bandwidth and Averaging

In the initial stages of the project, poor results were obtained for both frequency and spatial experiments. The problem was not with the experimental apparatus used, but with the resolution bandwidth (RBW) and averager of the spectrum analyzer. Since the intensity measurements fluctuate significantly from sample to sample the averager must be implemented to yield reliable results. Also, to obtain sensible results, the RBW of the spectrum analyzer must be selected appropriately to guarantee appropriate measurement sensitivity. The entire desired spectrum (4.8 GHz to 7.86 GHz) was naively chosen at first as the RBW, which sent the measured intensity peak levels nearly into the background noise. Needless to say this data was unusable and had to be retaken, greatly postponing objective deadlines.

Pick-up Antenna Selection

For the initial experiments, the receiver antenna we used produced signals which were not repeatable or reliable. Later experiments were done with a smaller receiver and repeatable and stable measurements were taken. This stability allowed us to gather the qualitative data needed to chose the correct antenna. For quantitative results it would be necessary to characterize the receiver antenna and include it as part of the overall system transfer function.

3. Conclusions

The characterization of the helical and dipole antenna at 6.8GHz, presented in the results section, provide a set of baseline data. This baseline data will be compared with data measured for the final design. Ideally, the final design will exhibit higher directivity than the two previous models.

It is concluded from the baseline data that the optimal antenna form, when choosing between a dipole antenna and a helical antenna, is the helical antenna. This antenna exhibits higher directivity, and with some changes to the design is tuned to the correct center frequency.

Research into alternative designs produced information on parasitic and array antennas, both of which are incorporated into the final design. The final version of the antenna is based on a helical antenna which is very similar to the current model; with a slightly smaller diameter and length resulting from the re-calculated dielectric constant of Delrin ($\varepsilon = 3.393$). Also, a parasitic wire is wound between the turns of the drive antenna to increase the directivity. Four antennas will be fabricated for the 6.8GHz model and the 3.0GHz model. These will be installed on a ground plate in a 2 by 2 array. The function of the array is to further increase the directivity and tune the input impedance to 50Ω. Plans have been submitted to the electrical machine shop for antenna fabrication.

Objective 4, characterization of the final design, is incomplete due to time constraints. Numerous sources contributed to this including RbSS troubleshooting and incorrect usage of the spectrum analyzer resolution bandwidth which resulted in the need to reacquire most of the data.

4. Recommendations

1. **Characterization of new antennas:** The procedure used to characterize the emission pattern and frequency dependency of each antenna should be done in a completely reproducible way. In general, the laboratory space used to perform these experiments is filled with objects which may cause reflections that alter measurements. It is important that the researcher be careful to arrange the antennas in the same fashion each time an experiment is performed to reduce the relative error incurred by the environment.

2. **Construction of new antennas:** Since the new antennas are meant to be placed in an array, the theory is based on the premise that they are identical (same input impedance and helical parameters). It is therefore necessary to construct each element in a similar fashion to optimize homogeneity.

3. **Selecting appropriate spectrum analyzer settings:** We had lost a lot of time collecting unusable data with the spectrum analyzer because the resolution bandwidth used was too large, creating intensity readings which were close to background noise level. Staying aware of which RBW is being used will lead to higher measurement sensitivity and reduction of errors. Also, since the signal encounters a large amount of noise traveling from the RbSS to the helical antenna, from the helical antenna to the receiver antenna, and finally from the receiver antenna to the spectrum analyzer, it is important to average over a reasonable time span (20 data points) to minimize outside-system influences on measurements.

4. **Characterization of receiver antenna:** Since our study was focused on obtaining information about the helical and dipole antennas *relative* to each other qualitatively, it was not imperative that the full system transfer function was known since the system is assumed to be linear time-invariant. When characterizing the final designs, however, the quantitative response of the antennas will be desired, and the receiver antenna will need to be characterized. This can be done by placing a fully characterized antenna on the output line of the RbSS and obtaining the signal through the receiver antenna into the spectrum analyzer. Then the system can be reversed, i.e. place the receiver antenna on the output line of the RbSS and the characterized antenna into the spectrum analyzer. The comparison of these two responses will allow the transfer function of the receiver antenna to be calculated.

Bibliography

1. **Robinson, Alan.** *Measuring the Molecular Structures of Ultracold Lithium-Rubidium Dimers by Feshbach Resonance.* Vancouver : University of British Columbia, 2009.

2. **Rybarczyk, Theo.** *Microwave system for 85-RB and 87-RB hyperfine transitions and Feshbach resonances.* Vancouver : University of British Columbia, 2009.

3. Our Technologies: Fractal Antenna Systems. [Online] Fractal Antenna Systems Inc. [Cited: September 25, 2009.] http://www.fractenna.com/index.html.

4. *Verification of Four Elements Helical Antennas Array Design Procedure.* **Zemanovic, Jan, Peter, Hajach and Podhoransky, Peter.** 2008.

5. **Kraus, John D.** *Antennas.* 2nd Edition. New York : McGraw-Hill, 1988. 0-07-463219-1.

6. *Applications of the Feshbach-resonance management to a tightly confined Bose-Einstein Condensate.* **Filetralla, Giovanni, Malomed, Boris A and Salasnich, Luca.** 4, April 2, 2009, Physical Review A, Vol. 79.

Appendix A – Dimensioned Drawings

6.8 GHz Prototype

Delrin Shell

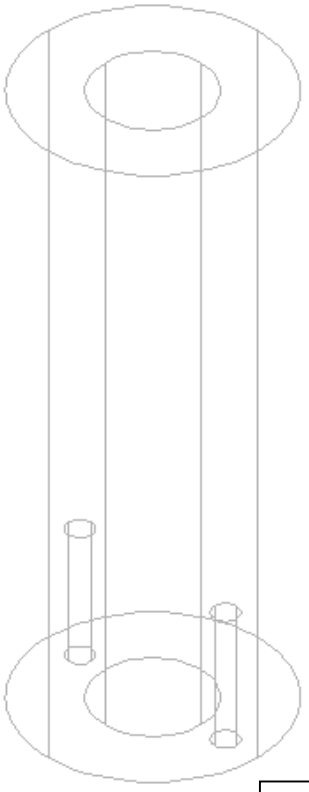

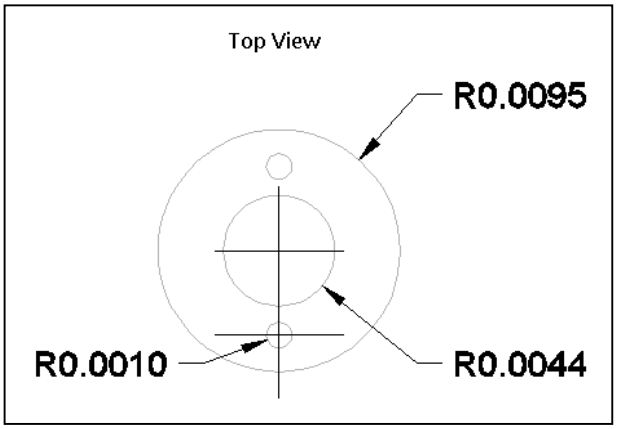

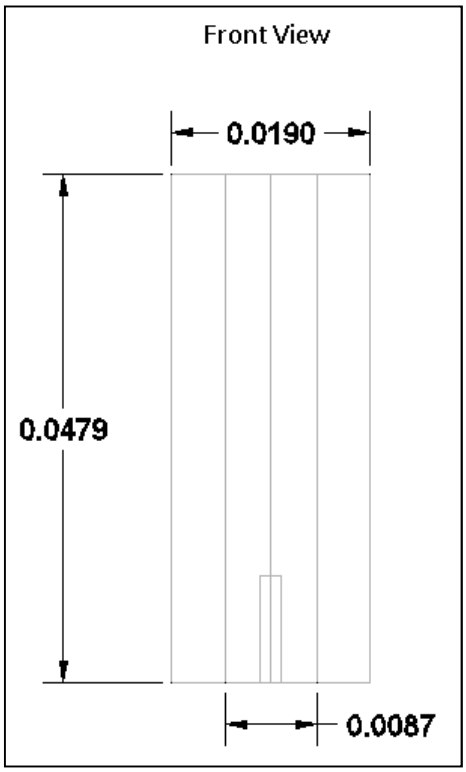

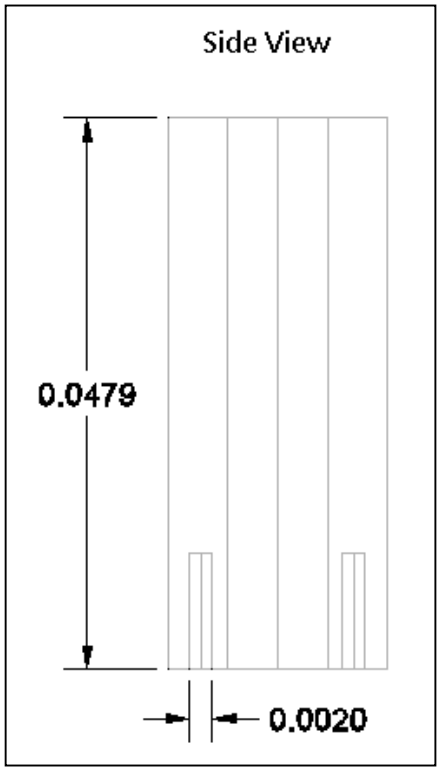

Delrin Core

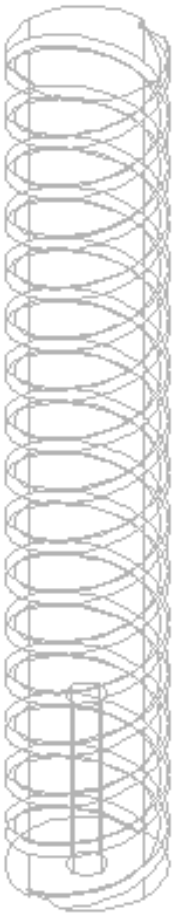

Helix Pitch Angle: 13.5° (8 turns)

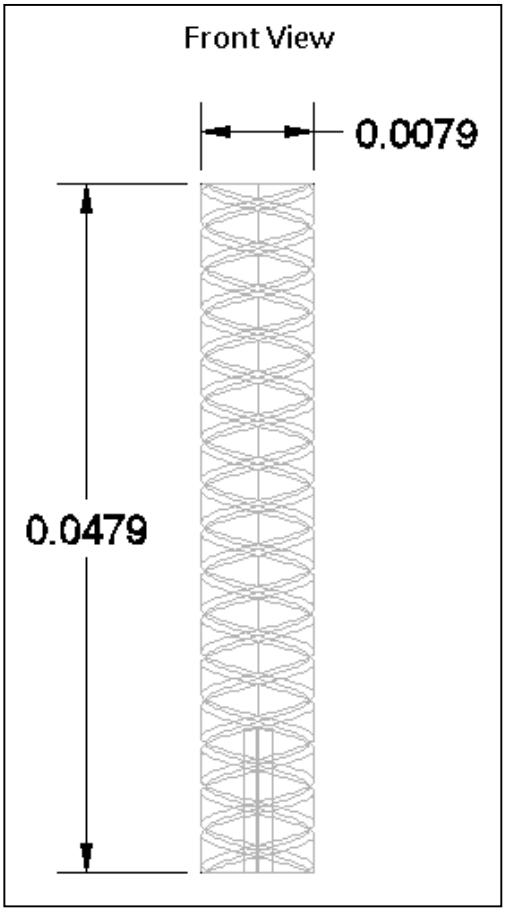

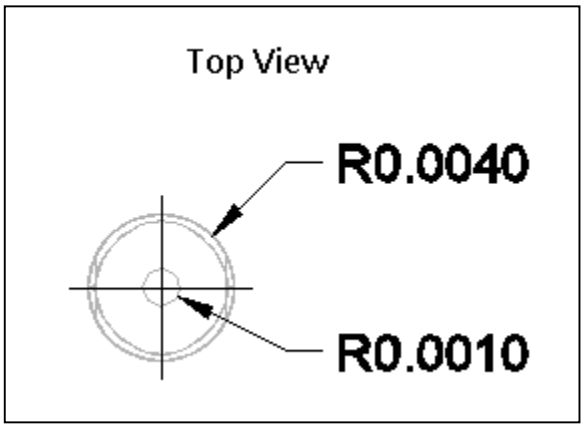

Copper Base

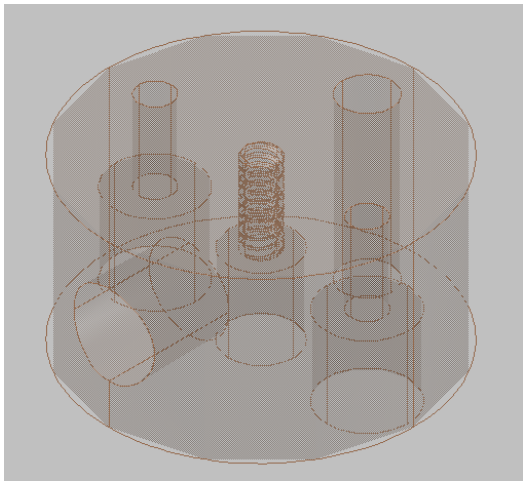

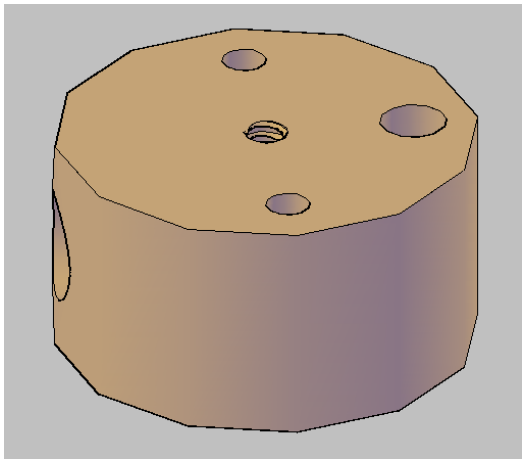

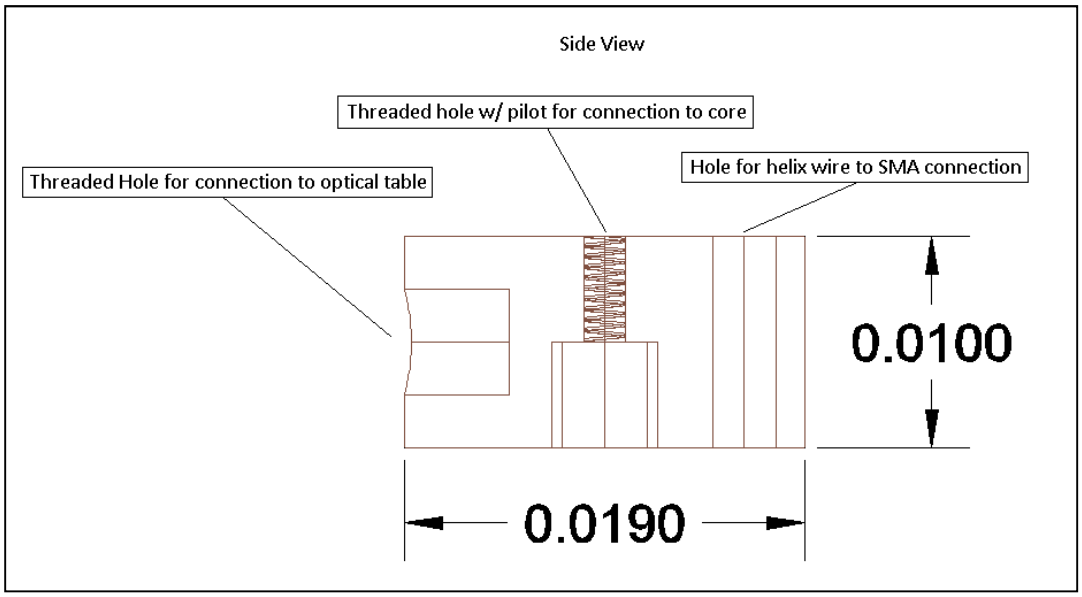
Side View
Threaded hole w/ pilot for connection to core
Hole for helix wire to SMA connection
Threaded Hole for connection to optical table
0.0100
0.0190

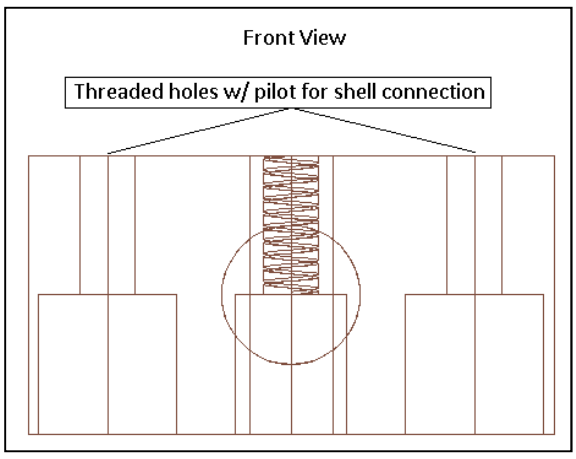
Front View
Threaded holes w/ pilot for shell connection

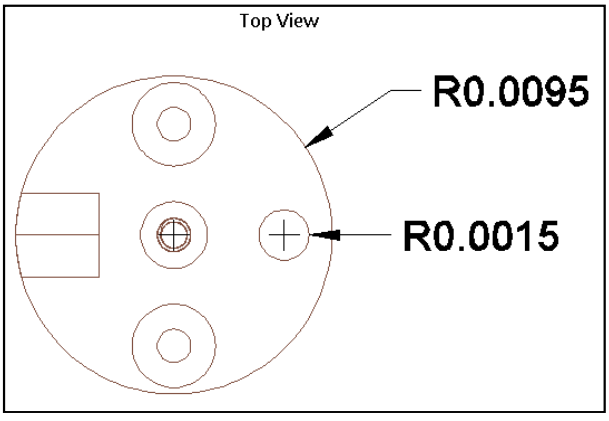
Top View
R0.0095
R0.0015

3.0 GHz Prototype

Delrin Shell

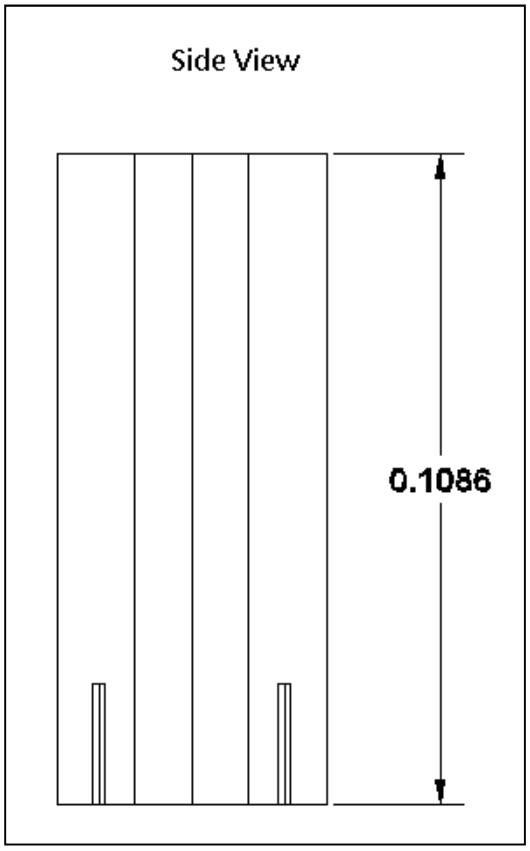

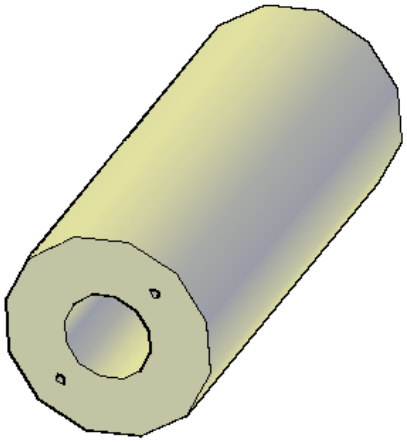

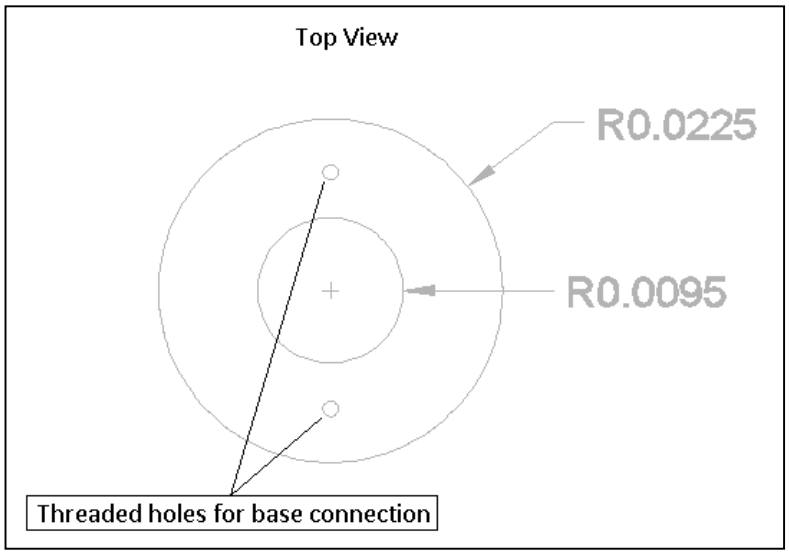

Delrin Core

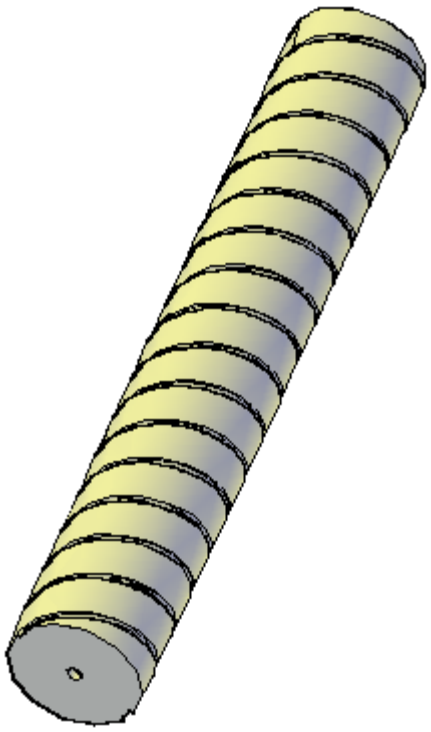

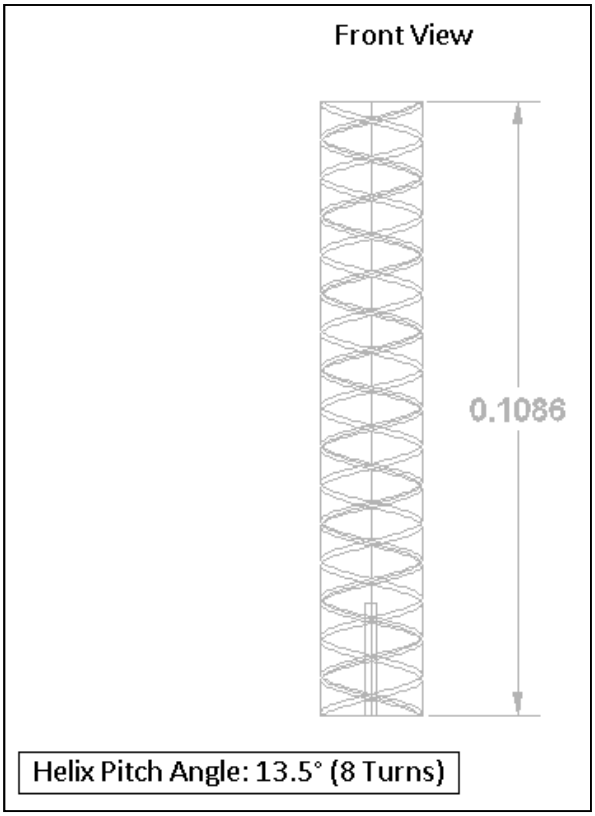
Front View
0.1086
Helix Pitch Angle: 13.5° (8 Turns)

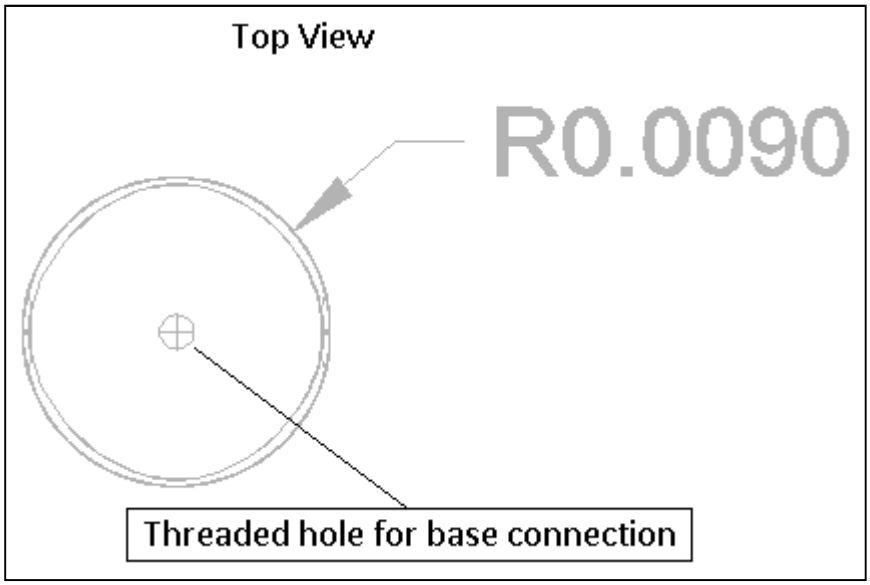
Top View
R0.0090
Threaded hole for base connection

Copper Base

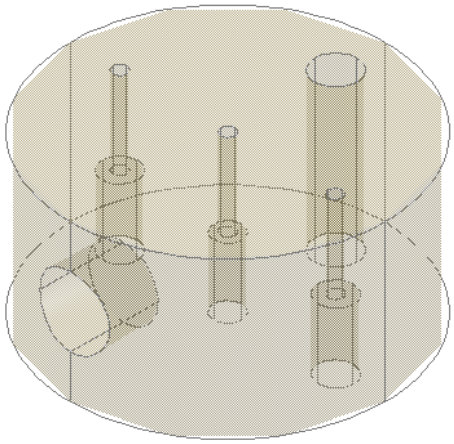

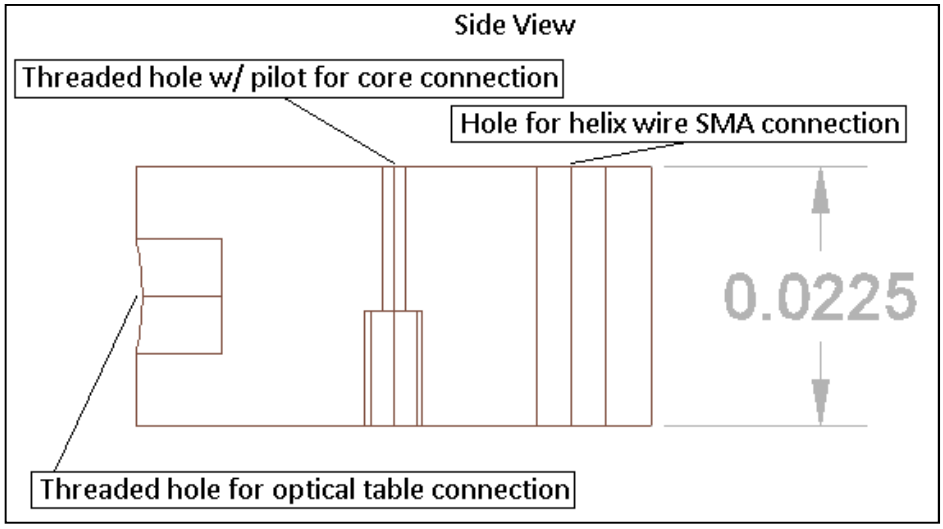
Side View
Threaded hole w/ pilot for core connection
Hole for helix wire SMA connection
0.0225
Threaded hole for optical table connection

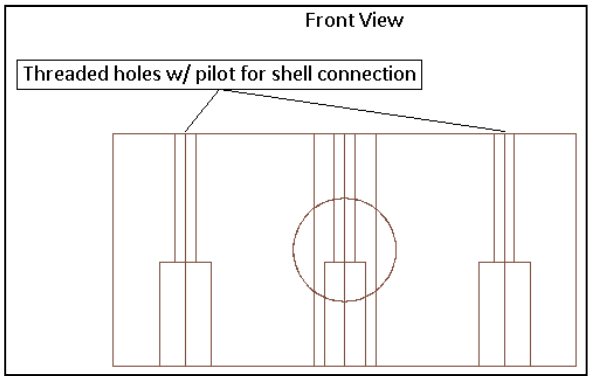
Front View
Threaded holes w/ pilot for shell connection

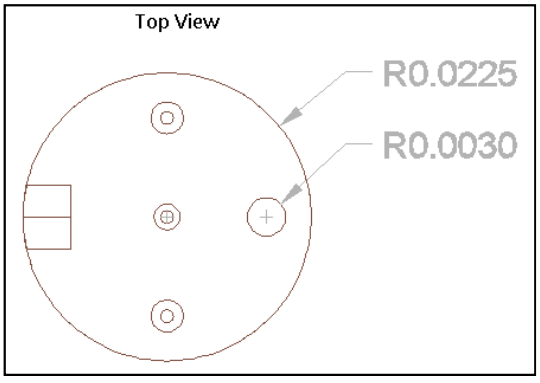
Top View
R0.0225
R0.0030

Appendix B – MATLAB Script for Trace Data Compilation

Helix.m

```
%%%%%%%%%%%%%%%%%%%%%%%%%%%%%
% This program imports Spatial Emission Pattern data
% and transcribes peak values to a 3D Grid. This
% particular file is defined FOR HELICAL ANTENNA
% assuming output symmetry
% Structure of Data Files:
%   Define the following alpha-to-numeric constants:
%                       A = 0
%                       B = 1
%                       C = 2
%                       D = 3
%                       E = 4
%                       F = 5
%                       G = 6
%                       H = 7
%                       I = 8
%                       J = 9
%       Name Format:     _  _  _  _.csv
%                       (1)(2)(3)(4)
%           Positions 1,2, and 3 specify the distance the receiving antenna
%           is placed from the emitting antenna, measured in centimeters
%                   For example:   BJD_.dat
%                                   would indicate that the receieving
%                                   antenna was placed 193 cm from emitting
%                                   antenna.
%           Position 4 incicates the angle the normal of the receiving
%           antenna makes with the negative of the normal of the emitting
%           antenna.
%           This is coded alphabetically as well:
%               S = 0
%               T = 45
%               U = 90
%               V = 135
%               W = 180
%               X = 225
%               Y = 270
%               Z = 315
%                   For example:   DABX.csv
%                                   would indicate the receiving antenna
%                                   was placed 301 cm away from the
%                                   emitting antenna with 225 degrees
%                                   between the normal of the receiving
%                                   antenna and the negative of the normal
%                                   of the transmitting antenna.
%%%%%%%%%%%%%%%%%%%%%%%%%%%%%%%%%%%%%%%%%%%%%%%%%%%%%%%%%%%%%%%%%%%%%%%
% Define Character Space for Spatial and Angular File-Specific Coordinates
SPC  =  ['A','B','C','D','E','F','G','H','I','J', '0'];
NSPC =  ['0','1','2','3','4','5','6','7','8','9'];
n = length(SPC);
ANG  =  ['S','T','U','V','W','X','Y','Z', '0'];
NANG =  ['000','045','090','135','180','225','270','315', '000'];
m = length(ANG);
counter = 0;
% Create all possible
% maxima(1,1) = 'frequency';
% maxima(1,2) = 'intensity';
% maxima(1,3) = 'distance';
% maxima(1,4) = 'angle';
for i = 1:m
     for j = 1:2
         for k = 1:n
```

```
            for l = 1:n
                temp = strcat(SPC(j), SPC(k), SPC(l), ANG(i),'.csv');
                if exist(temp)==0
                else
                counter=counter+1;
                M1 = csvread(temp, 15);
                data = M1(:,1:2);
                [C,I] = max(data(:,2));
                maxima(counter,1) = max(data(:,2));
                %Makes sure max is at 6.8 GHZ
                %maxima(counter,1) = data(I,1);
                tdist(counter,1) = {strcat(NSPC(j),NSPC(k),NSPC(l))};
                tang(counter,1) = {strcat(NANG(3*i-2),NANG(3*i-1),NANG(3*i))};
                clear M1 data;
                end
            end
        end
    end
end
% Now that all the data has been imported from csv files into matlab:
% Organize the files in terms of angles, and then in terms of distance


for i = 1:counter
    if strcmp(tang(i),'045')
        for j = 1:10
            tt = tdist{i*j};
            max45(1,j) = str2num(tt);
            max45(2,j) = maxima(i*j);
        end
        i = i + 10;
    elseif strcmp(tang(i),'090')
        for j = 1:10
            tt = tdist{i*j};
            max90(1,j) = str2num(tt);
            max90(2,j) = maxima(i*j);
        end
    i = i + 10;
    elseif strcmp(tang(i),'135')
        for j = 1:10
            tt = tdist{i*j};
            max135(1,j) = str2num(tt);
            max135(2,j) = maxima(i*j);
        end
        i = i + 10;
    elseif  strcmp(tang(i),'180')
        for j = 1:10
            tt = tdist{i*j};
            max180(1,j) = str2num(tt);
            max180(2,j) = maxima(i*j);
        end
        i = i + 10;
    elseif  strcmp(tang(i),'225')
        for j = 1:10
            tt = tdist{i*j};
            max225(1,j) = str2num(tt);
            max225(2,j) = maxima(i*j);
        end
        i = i + 10;
    elseif  strcmp(tang(i),'270')
        for j = 1:10
            tt = tdist{i*j};
```

```
            max270(1,j) = str2num(tt);
            max270(2,j) = maxima(i*j);
        end
        i = i + 10;
    elseif  strcmp(tang(i),'315')
        for j = 1:10
            tt = tdist{i*j};
            max315(1,j) = str2num(tt);
            max315(2,j) = maxima(i*j);
        end
        i = i + 10;
    elseif  strcmp(tang(i),'360')
        for j = 1:10
            tt = tdist{i*j};
            max360(1,j) = str2num(tt);
            max360(2,j) = maxima(i*j);
        end
        i = i + 10;
end
end
```

CONTOURPLOT.m

```
% Creates the contour plots used to analyze spatial emission patterns of 6.8GHz dipole and
helical %antennas
% Average the results of the angle tests

nHelix = (AngleHelix20(:,3)+AngleHelix30(:,3))/2;
nDipole = (AngleDipole20(:,3)+AngleDipole30(:,3))/2;

% Define Angle and Displacement values

T = [ 180 150 120 90 60 30 0 ];

D = [ 10 20 30 40 50 60 70 80 90 100 ];

for k = 1:length(T)

    for j = 1:length(D)
        x(j,k) = D(j)*cosd(T(k));
        y(j,k) = D(j)*sind(T(k));
    end

end

% Normalize the spatial vectors to the average of the angle tests

for i = 1:length(nHelix)
    h(:,i) = (DistanceHelix1(:,3) - nHelix(i));
end

for i = 1:length(nDipole)
    d(:,i) = DistanceDipole1(:,3) - nDipole(i);
end

h = flipud(h);
d = flipud(d);

subplot(1,2,1);contourf(x,y,h);
subplot(1,2,2);contourf(x,y,d);
clear i j;
```